4 September 1997

PHYSICS LETTERS B

ELSEVIER

Physics Letters B 407 (1997) 212–218

A measurement of the beta asymmetry A in the decay of free neutrons

H. Abele [a], S. Baeßler [a], D. Dubbers [a], J. Last [b], U. Mayerhofer [b], C. Metz [a], T.M. Müller [a], V. Nesvizhevsky [b], C. Raven [a], O. Schärpf [b], O. Zimmer [b]

[a] *Physikalisches Institut der Universität Heidelberg, Philosophenweg 12, D-69120 Heidelberg, Germany*

[b] *Institut Laue-Langevin, Avenue des Martyrs, F-38000 Grenoble, Switzerland*

Received 27 February 1997; revised manuscript received 3 June 1997
Editor: R.H. Siemssen

Abstract

We have measured the beta asymmetry A in the decay of free polarized neutrons, using the 4π superconducting spectrometer PERKEO II. The asymmetry parameter is $A_0 = -0.1189(12)$ corresponding to $g_A/g_V = -1.274(3)$. This value differs by three standard deviations from the one given by the Particle Data Group 1996. Our result contradicts earlier speculation on the existence of right-handed currents in neutron decay. © 1997 Elsevier Science B.V.

PACS: 12.30 13.30.ce; 14.20.Dh; 23.40.Bw

The decay of the neutron is a baryon semileptonic decay involving solely the first quark generation: A neutron transforms into a proton, an electron, and an electron antineutrino. The observables in neutron decay depend on the semileptonic weak coupling constants. A precise knowledge of these coupling constants probes the structure of the electroweak standard model at low energies. In the standard model only two parameters are needed to describe free neutron decay, namely

$$\lambda = \frac{g_A}{g_V}, \tag{1}$$

the ratio of axial vector to vector coupling constants, and V_{ud}, the first entry in the quark mixing matrix. We assume time reversal invariance, that is λ is a real number. In neutron decay about half a dozen observables are accessible to experiment, so the problem is strongly overdetermined and, together with other data from particle and nuclear physics, many tests of the standard model become possible [1–3].

Further, all semileptonic cross-sections used in cosmology, astrophysics and particle physics are based on neutron decay data. In particular free neutron decay measurements are the only means of precisely determining g_A. Also of current interest is that λ is related to the spin structure of the proton via the sum rule of Bjorken. Finally, the Goldberger–Treiman relation links g_A to the pion-nucleon-nucleon coupling constant, and the Adler–Weisberger relation links g_A to the pion-proton cross-section.

In 1990, all results from neutron decay were in agreement with the standard model [2]. Then in 1991, a new value of the beta asymmetry A, which is the correlation coefficient between the electron momentum and the neutron spin, was published [4]. The absolute value was significantly lower than in earlier measure-

PII S0370-2693(97)00739-9

Table 1
Results and prominent corrections in recent experiments on the beta asymmetry A.

Experiment:	PERKEO [11,12]	Erozolimskii et al. [4]	Schreckenbach et al. [8]	PERKEO II this work
year:	1986	1991	1995	1996
result:	−0.1146(19)	−0.1116(14)	−0.1160(15)	−0.1189(12)
corrections for:				
• magnetic mirror effect	13%	-	-	0.1%
• polarization	2.6%	27%	1.9%	1.5%
• solid angle	small	3%	15%	−0.24%
• background	~ 3%		~ 3%	1.55%

ments, see Table 1. This disagreement was frequently interpreted as a possible signature of the existence of right-handed currents in the weak interaction [5–7]. A more recent publication [8] on A, on the other hand, gave a value which was slightly higher than the previous values, so the situation was far from satisfactory. Here, we present a new measurement of the beta asymmetry A.

The differential decay probability per unit time for the emission of electrons from a polarized neutron beam is given by

$$dW = \left[1 + \frac{v}{c} PA \cos\theta\right] d\Gamma(E), \tag{2}$$

where v/c is the electron speed in units of the speed of light, θ is the electron emission angle relative to the direction of neutron polarization P, and $d\Gamma$ is the differential decay probability for unpolarized neutrons, which only depends on the electron kinetic energy E. The kinetic energy distribution $\Gamma(E)$ of electrons in neutron decay is given by the usual allowed distribution

$$\Gamma(E) = (E_0 - E)^2 (E + mc^2) \sqrt{E(E + 2mc^2)}, \tag{3}$$

where E and m are kinetic energy and mass of the electron, with an endpoint energy $E_0 = 781.6$ keV.

The values of $\Gamma(E)$ and A will be corrected for the Coulomb interaction, radiation and recoil effects, and also weak magnetism [19]. The relative variation of A with energy E due to these effects is about 1%. If we ignore them for now, the asymmetry parameter A is equal to

$$A_0 = -2 \frac{\lambda(\lambda + 1)}{1 + 3\lambda^2}. \tag{4}$$

In our experiment we measure the beta asymmetry by observing the difference in electron count rates as a function of electron energy E for two opposite neutron polarization states.

The instrument PERKEO II was installed at the PF1 cold neutron beam position at the european neutron source of the Institut Laue-Langevin, Grenoble. Cold neutrons are obtained from a 25 K deuterium cold moderator near the core of the 57 MW uranium reactor, and are guided via a 60 m long neutron guide of cross-section 6×12 cm^2 to our experiment.

Our experimental arrangement is sketched in Fig. 1. The neutrons are polarized by a supermirror polarizer over a cross section of 3×4.5 cm^2. The neutron polarization is reversed periodically with a current sheet spin flipper. The main component of the PERKEO II spectrometer is a superconducting 1.1 T magnet in a split pair configuration, with coil diameter of about one meter. About one out of 10^7 neutrons passing through the spectrometer decays within the spectrometer, and the decay electrons are guided by the magnetic field to either one of two scintillation detectors with photomultiplier readout.

The spectrometer field decreases monotonically from the center of the split pair to the detectors, insuring that electrons are not permanently trapped. The beta scintillation detectors are made from $440 \times 160 \times 5$ mm^3 Bicron BC 404. Each detector is coupled through light guides to two Hamamatsu R1332 photomultipliers operated in fast coincidence to reduce noise.

The experimental technique was already used by the predecessor of this experiment PERKEO I [9]: The detector solid angle of acceptance is $2 \times 2\pi$ and the energy threshold is 60 keV. Electron backscattering effects, serious sources of systematic error in beta-

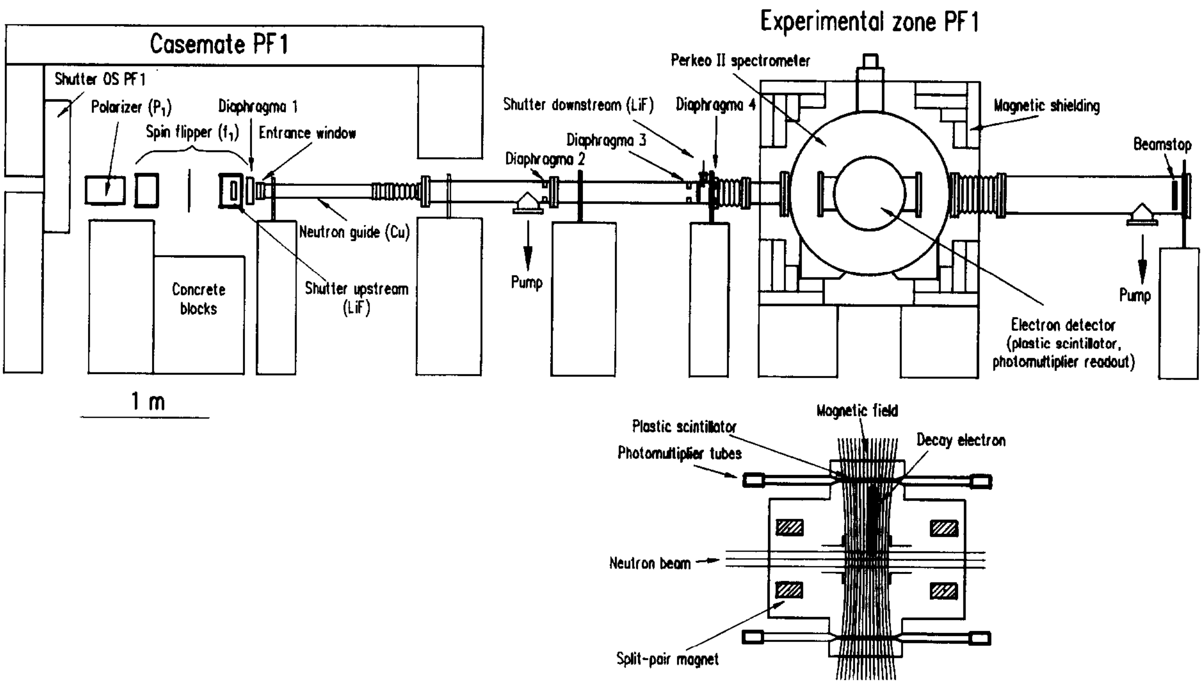

Fig. 1. Side view of the experimental setup. The sketch below shows the spectrometer itself in top view.

spectroscopy, are effectively suppressed. An electron which backscatters from one detector is either reflected back by the magnetic field or it follows a magnetic field line and eventually hits the other detector. About 3% of electrons hit both detectors. In that case the electron energy signal is derived from the sum of signals from both scintillators. By using time of flight information we determine which detector was hit first.

PERKEO II has a number of advantages over the old instrument. It uses a magnetic field, which is perpendicular to the cold neutron beam direction. As a consequence, the electron detectors are installed at a larger distance to the neutron beam, which reduces background significantly. The signal to background ratio in the range of interest is 20 : 1. Some decay electrons are reflected in the non-uniform magnetic field. In the new instrument this magnetic mirror effect is strongly reduced, see also Table 1.

The detector energy is calibrated with conversion electron sources on 5 μg/cm^2 carbon backings, which can be remotely inserted near the center of PERKEO II. The isotopes are ^{109}Cd, ^{139}Ce^{114m}In, ^{113}Sn, ^{85}Sr and ^{207}Bi, to cover the full β-energy range of neutron decay. We use a Poisson-like detector response function. The usual backscatter tail normally encountered in electron detectors is suppressed in our spectrometer, as already discussed. The detector response for an electron with energy E is about 236 keV $\sqrt{E[\mathrm{MeV}]}$ (FWHM). The neutron decay countrate is 330 s^{-1}.

Deviations from linearity of the energy-channel relation were no larger than 1%, but the straight line misses the ADC-pedestal by 22 keV due to non-linearities at low energies (below 70 keV) or due to a dead layer on the detector.

Since PERKEO has a $2 \times 2\pi$ acceptance, we must include the effect of detected Auger electrons. They shift the conversion electron peaks to higher energies. We investigated some of the calibration sources offline in great detail, by using silicon detectors with an energy resolution of 2 keV. For this investigation we did not use the full size neutron decay spectrometer PERKEO II but the smaller version PERKINO. No significant deviations from literature values were found. These investigations also led to stringent limits on neutrino masses in the 17 keV region [10].

The neutron polarization is reversed every 30 sec.

The efficiency of the polarizer (P_1) and the spinflipper (f_1) was determined with a new method: In the (conventional) first step [20] we installed a chopper, a second spinflipper (f_2), and a second polarizer (P_2) behind the exit window of the apparatus. By switching the spinflippers in various combinations we deduce $f_1(\lambda)$, $f_2(\lambda)$, and $P_1P_2(\lambda)$. Here, λ is the de Broglie wavelength of the neutron. Then we inserted another spinflipper (f_3) and a third polarizer (P_3) without moving the other components in order to avoid errors caused by the position dependence of the polarizers. We obtained the ratio of the efficiencies of the first and the second polarizer by switching the first and the third spinflipper:

$$\frac{P_2}{P_1}(\lambda) = 2f_1(\lambda) \times \frac{N^{\downarrow\downarrow}(\lambda) - N^{\downarrow\uparrow}(\lambda)}{N^{\downarrow\downarrow}(\lambda) - N^{\downarrow\uparrow}(\lambda) + N^{\uparrow\uparrow}(\lambda) - N^{\uparrow\downarrow}(\lambda)} - 1. \tag{5}$$

$N^{\downarrow\downarrow}(\lambda)$ is the count rate with f_1 and f_3 off, $N^{\uparrow\downarrow}(\lambda)$ the count rate with f_1 on and f_3 off, and so on. Then

$$P_1 = \int \sqrt{P_1P_2(\lambda)\frac{P_1}{P_2}(\lambda)}\Phi_c(\lambda)d\lambda \bigg/ \int \Phi_c(\lambda)d\lambda. \tag{6}$$

The capture flux

$$\Phi_c(\lambda) = \int \frac{\lambda}{\lambda_0}\frac{\partial\Phi}{\partial\lambda}d\lambda$$

with $\lambda_0 = 1.8$ Å is the equivalent thermal flux. Behind the exit window of our spectrometer the neutron beam intensity profile has approximately the shape of a trapezoid with a base line of 9 cm and a top line of 3 cm. At this position we measured the polarization at three equidistant points of the beam. The points were chosen on a horizontal line because of the horizontal curvature of the supermirrors. The results are in statistical agreement (97.16(35)%, 98.21(40)%, and 97.68(33)%). After small corrections to the capture flux spectrum, which take into account the resolution of the chopper and neutron scattering and absorbtion in air and in the vacuum window, we obtain $P_1 = 97.63(29)\%$. Unfortunately, after the end of the beam time we found out that the chopper worsened the polarization of the beam, most probably due to its Gd-coated metal disc, which caused rotating magnetic fields due to induction currents. As we do not know the size of this depolarization, this effect must be covered by the error of the polarization measurement. The effect could not have been more than 2.37%, as true polarization is lower than 100%. In fact, polarizations higher than 99% have never been observed with this kind of polarizer. We applied a depolarization correction of $+0.87(68)\%$ which leads to a neutron beam polarization of $P = P_1 = 98.50(78)\%$. The one sigma interval of polarization then is from 97.76% to 99.26%, that is a value of 100% polarization is still within our two sigma interval. The spinflip efficiency was measured to $f_1 = 99.17(14)\%$.

An unpolarized β-spectrum is shown in Fig. 2a. The background spectrum, which was subtracted from the data, is shown separately. Sources of background are γ radiation and electrons from Compton scattering and fast neutrons from ^{6}LiF [21]. The background consists of two parts. The first part was measured by blocking the neutron beam with a ^{6}LiF shutter after the polarizer (shutter upstream). This shutter is installed far away from the spectrometer and produces no additional background (see Fig. 1). We call this kind of background, which includes radiation from the reactor and the polarizer, the environmental background. If we subtract it from the data, we still find a small number of events well beyond the beta endpoint energy. This residual background is beam related background and originates from neutron capture in the ^{6}LiF diaphragm and in the beamstop. The scintillation detectors are shielded from these sources with lead, polyethylene and boron carbide and have no direct view onto them. Each γ ray that hits the detector must have undergone multiple scattering.

The shape of this beam-related background can be measured by blocking the beam with ^{6}LiF (shutter downstream) at the entrance of the spectrometer. This enhances the rate of beam related background coming from this part of the beamline, while the true neutron decay spectrum is suppressed. Further, we installed artificial γ and fast neutron sources (^{60}Co and Am/Be) at various positions of the beam line. We observed that the shape of all these background spectra was basically the same and without structure. Therefore it is justified to extrapolate the background spectrum observed above the beta endpoint energy into the fit interval from 325 keV to 675 keV. All uncertainties in

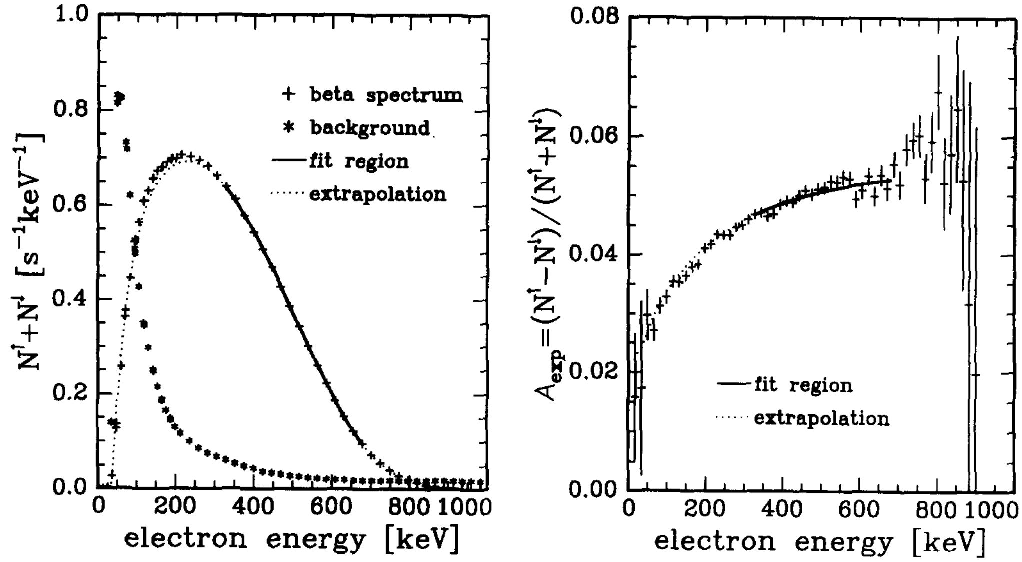

Fig. 2. Left: neutron beta spectrum. Cross: electron energy spectrum after adding opposite neutron spin orientations $N^{\uparrow}$ and $N^{\downarrow}$. Asterisk: background which was subtracted from the raw data. The solid line shows a fit in the energy range between 325 keV and 675 keV and the dotted line shows an extrapolation to lower energies. Right: neutron beta asymmetry. The solid line shows a fit to the experimental asymmetry $A_{\rm exp}$ and the dotted line shows an extrapolation to lower energies.

this extrapolation procedure are covered by the large error of 30% that we applied. The correction on A_0 due to this beam related background is 1.55(45)%.

Fig. 2a shows the fit of the theoretical spectrum to the background corrected data for this fit interval, and its extrapolation to lower energies. At lower energies a small deviation from the data points exists, which might be due to unsubtracted residual background.

The measured electron spectra $N_i^{\uparrow}(E)$ and $N_i^{\downarrow}(E)$ in the two detectors ($i = 1, 2$) for neutron spin up and down, respectively, define the experimental asymmetry as a function of electron kinetic energy

$$A_{\rm exp} = \frac{N_i^{\uparrow}(E) - N_i^{\downarrow}(E)}{N_i^{\uparrow}(E) + N_i^{\downarrow}(E)} . \tag{7}$$

From (2), with $\langle \cos\varphi \rangle = \frac{1}{2}$, we have

$$A_{\rm exp} = \frac{1}{2}\frac{v}{c} PA . \tag{8}$$

The recoil order and weak magnetism contributions to the asymmetry parameter A have the form

$$A = A_0(1 + A_{\mu\rm m}(A_1 W_0 + A_2 W + A_3/W)) , \tag{9}$$

with $W = E/mc^2 + 1$ (endpoint W_0). A_0 is defined in Eq. (4), and the coefficients $A_{\mu\rm m}$, A_1, A_2 and A_3 are taken from Wilkinson [13]. Additionally, a small radiative correction [19,13] is applied.

Table 2
Summary of our corrections to the raw asymmetry.

Effect	Correction	Uncertainty
neutron polarization:		
• measurement	+2.37%	0.29%
• correction due to chopper	−0.87%	0.68%
• efficiency of the spin flipper	+0.83%	0.14%
beam-related background	+1.55%	0.45%
statistics		0.42%
energy calibration:		
• gain factor		0.2%
• detector response function	+0.04%	0.12%
detector edge effect	−0.24%	0.1%
electron backscattering effects		0.09%
magnetic mirror effect	+0.10%	0.01%
variations of the neutron flux		0.05%
radiative corrections	+0.09%	0.01%

The asymmetry data, fitted again between 325 keV and 675 keV, with A_0 as the only parameter, are shown in Fig. 2b. After correcting for the polarization, spin flipper efficiency and other small effects listed in Table 2, we obtain $A_0 = -0.1189(12)$ and $g_A/g_V = -1.274(3)$. For every run we fitted each detector sep-

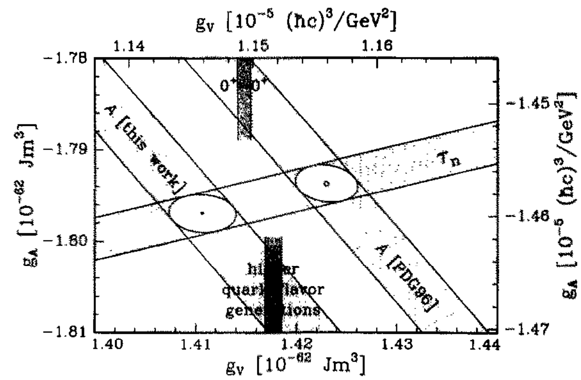

Fig. 3. g_A vs. g_V derived from measurements of the beta asymmetry A_0 and of the neutron lifetime τ_n. The shaded bands represent the one sigma error of the measurements. The intersection of both bands fixes each g_A and g_V to within one standard deviation, as shown by the error ellipse. Two different asymmetry values are displayed separately in this figure: the particle data group value, and our new value. Further, the g_V values derived from $0^+ \to 0^+$ nuclear β-decay [22] and from higher quark flavour decay [14], assuming the unitarity of the Cabibbo-Kobayashi-Maskawa matrix are also displayed.

arately. The average $\chi^2 = 153$ for 150 data point is found. The fit interval was chosen such that the signal-to-background ratio was at maximum. But the range of the fit interval has no significant influence on A_0. This gives us confidence in our background subtraction procedure.

Our new value A_0 differs by three standard deviations from the value $-0.1139(11)$ adopted by the particle data group in 1996 [14]. If we plot g_A and g_V, the neutron lifetime τ_n defines an ellipse, whereas the neutron decay asymmetry A_0 defines a straight line. Fig. 3 shows the intersection region of these lines. τ_n is an average of direct measurements of the neutron lifetime. The compilation comes from the particle data group, except for a value [23], which was withdrawn replaced by a newer one [15]. The shaded bands represent the one sigma error of the measurements. The intersection of both bands fixes g_A and g_V to within one standard deviation, which is indicated by the error ellipse. Two different asymmetry values are displayed separately in Fig. 3: the particle data group value, and our new value. Further, the g_V values derived from $0^+ \to 0^+$ nuclear β-decay [22] and from higher quark flavour decay [14], assuming the unitarity of the Cabibbo-Kobayashi-Maskawa mixing matrix are also displayed. Table 1 lists the A_0 data which significantly enter this analysis. Note that the maximum correction we had to apply to the raw asymmetry A_{exp} to obtain the final result A_0 is about one order of magnitude smaller than in all previous work, see Table 1.

Several recent evaluations of neutron decay data favoured the existence of a right-handed weak gauge-boson with a mass state m_2 between 207 GeV/c^2 and 369 GeV/c^2 at 95% C.L. [6]. In left-right symmetric models a left-handed W_L and right-handed W_R replace the left-handed W gauge boson of the standard model. W_L and W_R are combinations of two mass states W_1 and W_2 with masses m_1 and m_2 and a mixing angle ζ:

$$W_1 = W_L \cos\zeta - W_R \sin\zeta ,$$
$$W_2 = W_L \sin\zeta + W_R \cos\zeta . \qquad (10)$$

We here present a new evaluation of this question. We are interested in two of three parameters: first the mixing angle ζ and second the mass ratio squared between these two mass states

$$\delta = \left(\frac{m_1}{m_2}\right)^2 . \qquad (11)$$

Note that in the context of this model Eq. (4) is no longer valid. Instead, we take λ as a third free parameter. Fig. 4 shows an exclusion plot for δ and ζ due to a χ^2 analysis based on neutron decay data and $0^+ \to 0^+$ nuclear β-decay measurements. For each point in the plane the remaining parameter λ is optimized anew. The 70%, 90% and 95% C.L. contour lines are displayed. Fig. 4a shows the situation in 1991. The allowed region is not consistent with the standard model predictions $\delta = 0$ and $\zeta = 0$.

Fig. 4b shows the evaluation taking new neutron asymmetry data ([8] and this work) and new lifetime data [15–17] into account. In view of the large scatter of results for A_0, we increased all errors on A_0 by a scale factor 2.27. Additionally, we use a new value for the neutrino asymmetry coefficient B [18], which places better restrictions on δ. The new result is consistent with the standard model prediction on the one sigma level.

To summarize, we obtain $A_0 = -0.1189(12)$ and $g_A/g_V = -1.274(3)$. The corrections applied to our raw data are not larger than the quoted error. Our evaluation of all neutron decay data is consistent with the standard model of the electroweak interaction.

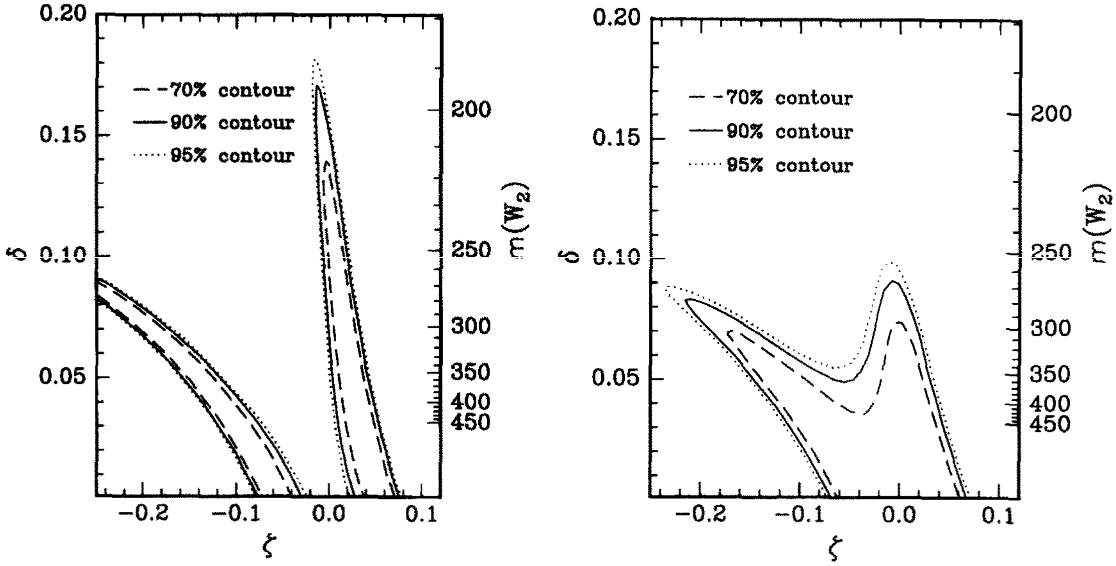

Fig. 4. Limits on right handed currents (inferred from neutron decay data and $0^+ \to 0^+$ nuclear β-decay measurements) are shown as countours in this plot of the mass ratio parameter δ vs. mixing angle ζ. The regions outside the contour lines are excluded with 70%, 90%, and 95% C.L., respectively. Left: status 1990: The standard model prediction for parameters $\delta = 0$ and $\zeta = 0$ are excluded by more than two signma. Right: status 1996. The result is consistent with the standard model prediction.

We thank S. Freedman for help in the early phase of the experiment, H. Börner and R. Günther for support during the measurements, J. Byrne for several additional days of beamtime, A.P. Serebrov for helpful discussions concerning polarization measurements, F. Glück for help with theoretical issues, and A. Pichlmayer for his work as a summer student.

This work has been funded by the German Federal Minister (BMBF) under contract number 06 HD 562 I.

References

[1] J. Deutsch et al., in: Precision Tests of the Standard Electroweak Model, edited by P. Langacker, World Scientific, 1995.
[2] D. Dubbers, Progr. Part. Nucl. Phys. 26 (1991) 173.
[3] D. Dubbers et al., Europhys. Lett. 11 (1990) 195.
[4] B.G. Erozolimskii et al., Phys. Lett. B 263 (1991) 33 and Sov. J. Nucl. Phys. 52 (1990) 999.
[5] Yu.V. Gaponov et al., Phys. Lett. B 253 (1991) 283.
[6] A.S. Carnoy et al., J. Phys. G 18 (1992) 823.
[7] N.B. Shul'gina, Phys. Rev. Lett. 73 (1994) 2658.
[8] K. Schreckenbach et al., Phys. Lett. B 349 (1995) 427.
[9] P. Bopp et al., Nucl. Instr. and Meth. A 267 (1988) 436.
[10] H. Abele et al., Phys. Lett. B 316 (1993) 26.
[11] P. Bopp et al., Phys. Rev. Lett. 56 (1986) 919.
[12] E. Klemt et al., Z. Phys. C 37 (1988) 179.
[13] D.H. Wilkinson, Nucl. Phys. A 377 (1982) 474.
[14] Particle Data Group, R.M. Barnett et al., Phys. Rev. D 54 (1996) 570.
[15] J. Byrne et al., Europhys. Lett. 33 (1996) 187.
[16] V.V. Nesvizhevskii et al., Sov. Phys. JETP 75 (1992) 405.
[17] W. Mampe et al., JETP Lett. 57 (1993) 82.
[18] I.A. Kuznetsov et al., JETP Lett. 60 (1994) 315.
[19] F. Glück et al., Phys. Rev. D 46 (1991) 2090. NB: in Table 5 the values for the beta asymmetry should be divided by a factor $(-\beta)$. (F. Glück, private communication, 1996).
[20] H. Kendrick et al., Nucl. Inst. Meth. 68 (1969) 50.
[21] M.A. Lone et al., Nucl. Instr. Meth. 174 (1980) 521.
[22] The ft values are taken from I.K. Towner et al., Proceedings of the ENAM-Conference, Arles (1995);
D.H. Wilkinson, Z. Phys. A348 (1994) 129;
W.E. Ormand et al., Phys. Rev. Lett. 62 (1989) 866.
[23] Byrne et al., Phys. Rev. Lett. 65 (1990) 289.